Astron. Astrophys. 293, 166–171 (1995)

ASTRONOMY AND ASTROPHYSICS

Line radiation cooling with partial redistribution in atmospheres with shocks

G. Hünerth and P. Ulmschneider

Institut für Theoretische Astrophysik der Universität Heidelberg, Im Neuenheimer Feld 561, D–69120 Heidelberg, Germany

Received 21 October 1993 / Accepted 30 January 1994

Abstract. We investigate the energy loss by spectral line radiation assuming partial redistribution PRD in atmospheres permeated by acoustic shock waves. It is found that with PRD the emission is much reduced and much more concentrated in a narrow region behind the shocks compared to cases which assume complete redistribution CRD. A fast method to approximate the radiation losses for time-dependent calculations is proposed.

Key words: methods: numerical – Sun: chromosphere – shock waves – radiative transfer – stars: atmospheres

1. Introduction

The assumption of complete redistribution (CRD) in the treatment of radiation transport in spectral lines yields energy loss rates which are often wrong by more than orders of magnitude (E.H. Avrett 1986, private communication, see below Sect. 3.1). This severely falsifies theoretical computations both of static atmospheres and of wave phenomena in the outer stellar atmospheres, because the vastly overestimated radiative loss rates lead to excessive mechanical heating requirements for empirically determined chromospheric temperature distributions as well as for the time-dependent chromospheric modelling. It is the purpose of the present work to show that by computing the radiation loss assuming partial redistribution (PRD), these loss rates are greatly diminished. In addition, the use of PRD significantly changes the physics of radiation cooling in atmospheres where shocks are present, because the cooling is found to be much more narrowly concentrated in the hot region immediately behind the shock, which is very different from the CRD case, where the radiation is spread over a large post-shock region. The computations of lines using PRD is performed with a new operator splitting method by Ulmschneider (1994).

This method, however, is too time consuming to work in time-dependent calculations, where the radiation loss of the atmosphere must typically be evaluated several thousand times in the course of a computational run. It is thus necessary to develop an approximation method, which on the one hand allows a much faster evaluation of the radiation loss, and on the other hand retains reasonable accuracy. This is found in a procedure which uses a CRD computation, where the damping wings of the line are artificially curtailed.

In Sect. 2 the radiation treatment is briefly described. Sect. 3 shows our results for static atmospheres and for several atmospheres permeated by acoustic shock waves. This section also outlines our proposed fast radiation loss method. Conclusions are presented in Sect. 4.

Send offprint requests to: P. Ulmschneider

2. Method

2.1. Radiative transfer

To discuss our radiation treatments and approximations we summarize the basic equations. For a spectral line with background continuum the transfer equation may be written

$$\mu \frac{\partial I_{\nu\mu}(\tau)}{\partial \tau} = \left[\varphi_{\nu\mu}(\tau) + r(\tau)\right]\left[I_{\nu\mu}(\tau) - S_{\nu\mu}(\tau)\right] \quad , \tag{1}$$

where

$$\tau(z) = \int_z^\infty \chi_L(z')dz' \quad , \tag{2}$$

is the reference (line center) optical depth and

$$r(z) = \frac{\chi_C(z)}{\chi_L(z)} \quad , \tag{3}$$

is the ratio of background to line center opacities. z is the geometrical height and $I_{\nu\mu}$ the specific monochromatic intensity of a beam of radiation inclined by an angle ϑ with respect to the outwardly directed z- axis. $\mu = \cos\vartheta$ and ν is the frequency. χ_L and χ_C are frequency-independent line and continuum opacities. $\varphi_{\nu\mu}$ is the absorption profile, given by the Voigt function

$$\varphi_{\nu\mu} = \frac{H(a,v)}{\sqrt{\pi}\Delta\nu_D} \quad , \tag{4}$$

with

$$a = \frac{\Gamma}{4\pi\Delta\nu_D} \quad , \tag{5}$$

$$v = \frac{\nu - \nu_0\left(1 - \mu\, u(z)/c_L\right)}{\Delta\nu_D} \quad . \tag{6}$$

Γ is the damping constant, $\Delta\nu_D$ the thermal Doppler width, u the gas velocity and c_L the light velocity. The absorption profile satisfies the normalisation condition

$$\int_{-1}^{1}\int_{-\infty}^{\infty} \varphi_{\nu\mu} d\nu d\mu = 1 \quad . \tag{7}$$

The total source function is given by

$$S_{\nu\mu}(\tau) = \frac{\varphi_{\nu\mu}(\tau) S^L_{\nu\mu}(\tau) + r(\tau)B(\tau)}{\varphi_{\nu\mu}(\tau) + r(\tau)} \quad , \tag{8}$$

where B is the Planck function and S^L the line source function given by (e.g. Cheng 1992)

$$S^L_{\nu\mu}(\tau) = [1-\epsilon(\tau)]\frac{1}{\varphi_{\nu\mu}(\tau)}\int_{-\infty}^{+\infty}\int_{-1}^{+1} R(\nu,\mu,\nu',\mu',\tau) \times I_{\nu'\mu'}(\tau)d\mu' d\nu' + \epsilon(\tau)B(\tau) \tag{9}$$

where

$$\epsilon(\tau) = \frac{\epsilon'(\tau)}{1+\epsilon'(\tau)} \; ; \; \epsilon'(\tau) = \frac{n_e(\tau)\Omega_{21}(\tau)}{A_{21}}\left(1 - \mathrm{e}^{-h\nu/kT(\tau)}\right), \tag{10}$$

is the photon destruction probability and R is the redistribution function. For ϵ and R see Mihalas (1978) Chap. 11 and 13. For R we take either the redistribution function R_{II} if we consider PRD or $\varphi_{\nu\mu}\varphi_{\nu'\mu'}$ when CRD is considered (see e.g. Mihalas 1978, Eq. 13–73). Note that in the CRD case the source function $S^L_{\nu\mu}$ becomes independent of ν and μ.

We restrict ourselves to two beams along the ray $\mu = \cos\vartheta$ (Ulmschneider 1994), where we have ingoing $I^-_{\nu\mu}(\tau)$ and outgoing $I^+_{\nu\mu}(\tau)$ photons, and where from now on $\mu = |\mu|$. For a more general description using more beams see Buchholz & Ulmschneider (1994). In the two beam approximation Eq. (1) can be written

$$\mu\frac{\partial I^+_\nu(\tau)}{\partial\tau} = \left[\varphi^+_{\nu\mu}(\tau) + r(\tau)\right]\left[I^+_\nu(\tau) - S^+_\nu(\tau)\right] \quad , \tag{11}$$

$$-\mu\frac{\partial I^-_\nu(\tau)}{\partial\tau} = \left[\varphi^-_{\nu\mu}(\tau) + r(\tau)\right]\left[I^-_\nu(\tau) - S^-_\nu(\tau)\right] \quad , \tag{12}$$

where τ after Eq. (2) does not depend on direction. The total source functions are then given by

$$S^+_\nu(\tau) = \frac{\varphi^+_{\nu\mu}(\tau)S^{L+}_{\nu\mu}(\tau) + r(\tau)B(\tau)}{\varphi^+_{\nu\mu}(\tau) + r(\tau)} \quad , \tag{13}$$

$$S^-_\nu(\tau) = \frac{\varphi^-_{\nu\mu}(\tau)S^{L-}_{\nu\mu}(\tau) + r(\tau)B(\tau)}{\varphi^-_{\nu\mu}(\tau) + r(\tau)} \quad . \tag{14}$$

Defining

$$G(\nu,\mu,\nu',\mu',\tau) \equiv \frac{R(\nu,\mu,\nu',\mu',\tau)}{\varphi_{\nu\mu}(\tau)} \quad , \tag{15}$$

the line source functions are written

$$S^{L+}_{\nu\mu}(\tau) = [1-\epsilon(\tau)]\int_{-\infty}^{+\infty} G(\nu,\mu,\nu',\mu',\tau)I^+_{\nu'\mu'}(\tau)d\nu' +$$

$$[1-\epsilon(\tau)]\int_{-\infty}^{+\infty} G(\nu,\mu,\nu',-\mu',\tau)I^-_{\nu'\mu'}(\tau)d\nu' + \epsilon(\tau)B(\tau) \quad . \tag{16}$$

$$S^{L-}_{\nu\mu}(\tau) = [1-\epsilon(\tau)]\int_{-\infty}^{+\infty} G(\nu,-\mu,\nu',\mu',\tau)I^+_{\nu'\mu'}(\tau)d\nu' +$$

$$[1-\epsilon(\tau)]\int_{-\infty}^{+\infty} G(\nu,-\mu,\nu',-\mu',\tau)I^-_{\nu'\mu'}(\tau)d\nu' + \epsilon(\tau)B(\tau) \; . \tag{17}$$

As the number of photons must be conserved during the scattering process we must require that

$$\int_{-\infty}^{+\infty} G(\nu,\mu,\nu',\mu',\tau)d\nu' + \int_{-\infty}^{+\infty} G(\nu,-\mu,\nu',\mu',\tau)d\nu' = 1 \quad , \tag{18}$$

$$\int_{-\infty}^{+\infty} G(\nu,\mu,\nu',-\mu',\tau)d\nu' + \int_{-\infty}^{+\infty} G(\nu,-\mu,\nu',-\mu',\tau)d\nu' = 1. \tag{19}$$

We now assume that the redistribution functions G are not strongly μ-dependent and that the μ-dependence enters the problem only, because it Doppler shifts frequencies due to the thermal motion of the gas particles and of the macroscopic fluid motion. In Eqs. (16), (17), photons with ν', μ' enter a gas element, are scattered and emerge with ν, μ. Here μ either remains unchanged or photons are scattered into $-\mu$. This allows to drop the μ- dependence in the G-functions except where it influences the frequencies ν.

Consider the scattering process in a gas element moving with the velocity u in $+z$-direction. Figure 2 of Ulmschneider (1994) shows the possible scattering processes. Following

a photon from the laboratory frame into the comoving frame of the gas element where it suffers a scattering event and reemerges Doppler shifted back in the laboratory frame, we have the four cases

$$\begin{aligned} G^{++}(\nu,\nu',\tau) &= G(\nu-\nu_0-\nu_0\frac{u\mu}{c_L},\nu'-\nu_0-\nu_0\frac{u\mu}{c_L},\tau)\\ G^{+-}(\nu,\nu',\tau) &= G(\nu-\nu_0+\nu_0\frac{u\mu}{c_L},\nu'-\nu_0-\nu_0\frac{u\mu}{c_L},\tau)\\ G^{-+}(\nu,\nu',\tau) &= G(\nu-\nu_0-\nu_0\frac{u\mu}{c_L},\nu'-\nu_0+\nu_0\frac{u\mu}{c_L},\tau)\\ G^{--}(\nu,\nu',\tau) &= G(\nu-\nu_0+\nu_0\frac{u\mu}{c_L},\nu'-\nu_0+\nu_0\frac{u\mu}{c_L},\tau) \end{aligned} \quad . (20)$$

With these redistribution functions the source functions (16), (17) are greatly simplified.

Integrating Eqs. (11), (12) one has the formal solution

$$\begin{aligned} I_\nu^+(\tau) &= \int_\tau^{\tau_N}\left[\varphi\left(\tau',\nu-\nu_0\frac{u(\tau')\mu}{c_L}\right)+r(\tau')\right]S_\nu^+(\tau')\\ &\cdot\exp\left\{-\int_\tau^{\tau'}\left[\varphi\left(\tau'',\nu-\nu_0\frac{u(\tau'')\mu}{c_L}\right)+r(\tau'')\right]\frac{d\tau''}{\mu}\right\}\frac{d\tau'}{\mu}\\ &+I_\nu^+(\tau_N)\exp\left\{-\int_\tau^{\tau_N}\left[\varphi\left(\tau'',\nu-\nu_0\frac{u(\tau'')\mu}{c_L}\right)\right.\right.\\ &\left.\left.+r(\tau'')\right]\frac{d\tau''}{\mu}\right\} \end{aligned} \quad (21)$$

$$\begin{aligned} I_\nu^-(\tau) &= -\int_0^{\tau}\left[\varphi\left(\tau',\nu-\nu_0\frac{u(\tau')\mu}{c_L}\right)+r(\tau')\right]S_\nu^-(\tau')\\ &\cdot\exp\left\{\int_{\tau'}^{\tau}\left[\varphi\left(\tau'',\nu-\nu_0\frac{u(\tau'')\mu}{c_L}\right)+r(\tau'')\right]\frac{d\tau''}{\mu}\right\}\frac{d\tau'}{\mu}\\ &+I_\nu^-(\tau_1)\exp\left\{\int_0^{\tau}\left[\varphi\left(\tau'',\nu-\nu_0\frac{u(\tau'')\mu}{c_L}\right)\right.\right.\\ &\left.\left.+r(\tau'')\right]\frac{d\tau''}{\mu}\right\} \end{aligned} \quad . (22)$$

Here $I_\nu(\tau_1)$, $I_\nu(\tau_N)$ are boundary intensities which can be set equal to zero if one has no incident radiation at the surface τ_1 and if the optical depth at the bottom τ_N is very large. The profile function $\varphi_{\nu\mu}$ has been written explicitly.

With N_τ depth and N_ν frequency points Eqs. (16), (17) can be written as matrix equations, where the number of subscripts indicates the size of the matrices

$$\mathbf{S}_{\nu\tau}^+ = \mathbf{R}_{\nu\nu'\tau}^{++}\mathbf{I}_{\nu'\tau}^+ + \mathbf{R}_{\nu\nu'\tau}^{+-}\mathbf{I}_{\nu'\tau}^- + \epsilon_\tau\mathbf{B}_{\nu\tau} \quad , \quad (23)$$

$$\mathbf{S}_{\nu\tau}^- = \mathbf{R}_{\nu\nu'\tau}^{-+}\mathbf{I}_{\nu'\tau}^+ + \mathbf{R}_{\nu\nu'\tau}^{--}\mathbf{I}_{\nu'\tau}^- + \epsilon_\tau\mathbf{B}_{\nu\tau} \quad , \quad (24)$$

where for every depth point τ, ϵ_τ is a scalar function and the **B** are vectors of size N_ν with the identical values of the Planck function at line center ($\nu=\nu_0$) as components. Here

$$\begin{aligned} \mathbf{R}_{\nu\nu'\tau}^{++} &\equiv (1-\epsilon_\tau)\mathbf{W}\mathbf{G}_{\nu\nu'\tau}^{++}\\ \mathbf{R}_{\nu\nu'\tau}^{+-} &\equiv (1-\epsilon_\tau)\mathbf{W}\mathbf{G}_{\nu\nu'\tau}^{+-}\\ \mathbf{R}_{\nu\nu'\tau}^{-+} &\equiv (1-\epsilon_\tau)\mathbf{W}\mathbf{G}_{\nu\nu'\tau}^{-+}\\ \mathbf{R}_{\nu\nu'\tau}^{--} &\equiv (1-\epsilon_\tau)\mathbf{W}\mathbf{G}_{\nu\nu'\tau}^{--} \end{aligned} \quad , \quad (25)$$

where **W** is a diagonal matrix of size $N_\nu\times N_\nu$ which contains the frequency integration weights. For every depth point τ, **I** and **S** are vectors of length N_ν and **R** matrices of size $N_\nu\times N_\nu$. For the formal solution one similarly finds

$$\mathbf{I}_{\nu'\tau}^+ = \Lambda_{\nu'\tau\tau'}^+\mathbf{S}_{\nu'\tau'}^+ \quad , \quad (26)$$

$$\mathbf{I}_{\nu'\tau}^- = \Lambda_{\nu'\tau\tau'}^-\mathbf{S}_{\nu'\tau'}^- \quad , \quad (27)$$

where the Λ-operator is a matrix of size $N_\tau\times N_\tau$ for every frequency point ν'. Equations (23) to (27) are not solved directly but we use the operator splitting method of Ulmschneider (1994).

2.2. The cooling rates

Integrating Eq. (1) over ν and μ gives the net radiative cooling rate ($erg/cm^3\ s$)

$$\Phi = \frac{dF}{dz} = \frac{d}{dz}2\pi\int_{-\infty}^{+\infty}\int_{-1}^{+1}I_{\nu\mu}(\tau)\mu d\mu d\nu$$

$$= -2\pi\chi_L\int_{-\infty}^{+\infty}\int_{-1}^{+1}\left[\varphi_{\nu\mu}(\tau)+r(\tau)\right]\left[I_{\nu\mu}(\tau)-S_{\nu\mu}(\tau)\right]d\mu d\nu \quad , (28)$$

which for our two beam approximation can be written

$$\begin{aligned} \Phi = 2\pi\chi_L\int_{-\infty}^{+\infty}&\left\{\left[\varphi_{\nu\mu}^+(\tau)+r(\tau)\right]\left[S_\nu^+(\tau)-I_\nu^+(\tau)\right]\right.\\ &\left.+\left[\varphi_{\nu\mu}^-(\tau)+r(\tau)\right]\left[S_\nu^-(\tau)-I_\nu^-(\tau)\right]\right\}d\nu \end{aligned} \quad . \quad (29)$$

3. Results

3.1. The Vernazza et al. model

As a first test we tried our methods on the well documented solar model C of Vernazza et al. (1981, hencefourth called VAL). The computed cooling rates Φ of the Mg II k line assuming PRD or CRD for this model are shown in Fig. 1. For the data used for the line Mg II k see Kalkofen et al. (1984). The PRD cooling rates are computed using the procedure discussed above (see also Ulmschneider 1994) while the CRD rates are evaluated with the method of Buchholz et al. (1994). Because the cooling rates vary over several orders of magnitude and also change signs we have used a modified logarithmic presentation which allows to

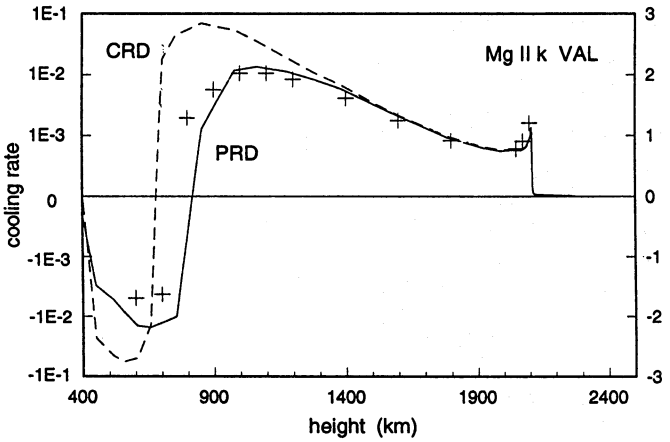

Fig. 1. Cooling rates Φ $(erg/cm^3 s)$ versus height for the solar model C of Vernazza et al. (1981), assuming PRD or CRD computed with our two level atom, two beam approximation methods. Values by Vernazza et al. are indicated by + symbols. The right hand axis indicates the logarithmic cooling rate C after Eq. (30)

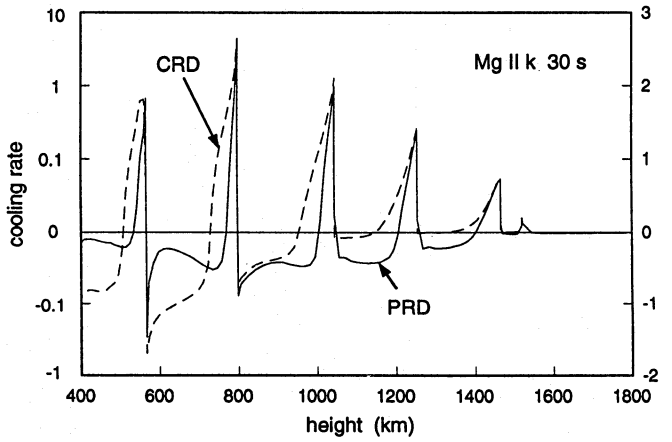

Fig. 2. Cooling rates Φ $(erg/cm^3 s)$ versus height for a solar acoustic wave model of initial energy flux $F_M = 2.0 \cdot 10^8$ $erg/cm^2 s$ and period $P = 30$ s shown in Fig. 7a of Rammacher & Ulmschneider (1992), assuming PRD or CRD computed with our two level atom, two beam aproximation methods. The right hand axis indicates the logarithmic cooling rate C after Eq. (30)

show the rates in a continuous manner. For this reason we plot the quantity C

$$C = \begin{cases} \log(A\Phi + 1) & , \text{if } \Phi > 0 \\ -\log(-A\Phi + 1) & , \text{if } \Phi < 0 \end{cases} , \qquad (30)$$

where $A = 10^4$. The scale of the quantity C is shown on the right hand axis, the left hand axis gives Φ itself. The PRD cooling rates agree quite well with the VAL values which were taken from Fig. 49 of Vernazza et al. (1981) and are indicated in Fig. 1. The discrepancies seen at lower height are attributed to our restriction to a two level atom representation. The striking feature of Fig. 1 is the large deviation of the CRD cooling rate from the PRD rate in the lower and middle chromosphere. At greater height the CRD rate becomes more and more equal to the PRD rate. This behaviour of the CRD rates is well known (E.H. Avrett 1986, who ran his VAL model using CRD on our request, private communication).

At great height the atmospheric density drops to such low values that only the Doppler core of the line has enough atoms to emit photons which contribute to the cooling. At these heights the assumption of complete redistribution is correct and CRD and PRD give the same rates. However, deep in the atmosphere the CRD assumption breaks down as it wrongly allows photons to be emitted far in the damping wings, while in reality the wing photons there suffer strict coherent scattering which does not contribute to the line cooling.

3.2. The acoustic wave calculations

We now turn to our acoustic wave calculations. Figures 2 and 3 show the Mg II k cooling rates Φ both for PRD and CRD for two solar acoustic wave calculations with initial energy fluxes $F_M = 2.0 \cdot 10^8$ $erg/cm^2 s$ and periods $P = 45$ and 30 s. The wave phases used here are shown in Figs. 1, 2 and 7a of Rammacher & Ulmschneider (1992), to which work we refer for a more detailed description of the wave phases. Similar as in the last subsection we plot also a logarithmic cooling rate C, after Eq. (30) with $A = 10^2$.

Again it is seen that there are large discrepancies between the PRD and CRD results. Both PRD and CRD cooling rates show a property seen in all of our previous wave calculations (e.g. Rammacher & Ulmschneider 1992) that the largest loss rates occur behind the shocks. The height-integrated line cooling in the CRD case is much larger than in the PRD case. This is mainly due to the fact that in PRD the cooling rates are concentrated much more in a narrow region behind the shocks, while in CRD the cooling is spread over a much larger height interval.

It is interesting that precisely in the post shock region immediately behind the shock the discrepancies between PRD and CRD are smallest (the rates at the hot sides of the shocks agree to better than 20%). From Rammacher & Ulmschneider (1992) it is known that due to the velocity jump the hot regions behind the shock are strongly Doppler shifted to the violet part of the spectrum and that thus the red shifted region in front of the shock has essentially negligible opacity for outgoing radiation at these violet wavelengths. The violet shifted hot post shock region can thus freely emit photons into the cool optically thin front shock region, that is, the shock discontinuity acts like a surface. CRD and PRD cooling rates are the same immediately behind the shock, because near a surface the complete redistribution assumption over the Doppler core is valid as was already found in the VAL case. Note that the photons emitted into the front shock region act to radiatively heat this region.

At greater distance from the shock in the post shock region the cooling rates again greatly deviate frome each other. Here the CRD assumption breaks down once more as the photons are coherent outside the Doppler core. The physical situation is very similar as in the VAL case described above. The shocks

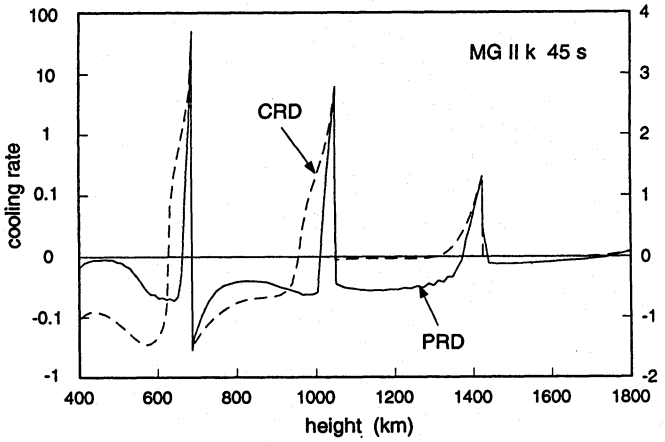

Fig. 3. Same as Fig. 2, however for a wave of period $P = 45\ s$. The wave phase is shown in Figs. 1, 2 of Rammacher & Ulmschneider (1992)

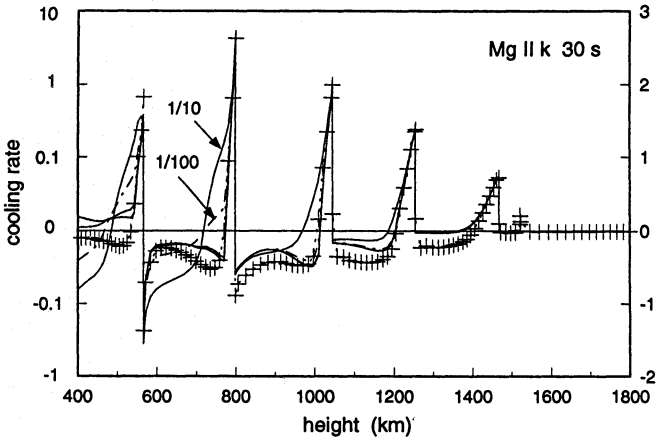

Fig. 4. Same as Fig. 2, however for damping parameters a of Eq. (5) multiplied by factors $1/10, 1/100, 1/1000, 0$. The PRD rates are shown dotted and with + symbols

act as internal surfaces and the CRD assumption breaks down at large distances from the surfaces.

3.3. Approximate simulation of PRD cooling

Figures 1 to 3 indicate that the emission in the core region of the line is most important for the PRD cooling rates and that immediately behind the shocks the PRD and CRD rates agree rather well. We are looking for an approximation of this property in the framework of a CRD calculation. For this reason we have followed a suggestion of R.J. Rutten (1988, private communication, based on an earlier finding of Caccin et al. 1977) and have computed cooling rates assuming CRD, but using an artificially reduced damping parameter a. A similar procedure seems to have been followed by Carlsson & Stein (1992). Figures 4 and 5 show CRD cooling rates where a in Eq. (5) is multiplied by $1/10$, $1/100$, $1/1000$ and 0 together with the PRD cooling rate indicated dashed as well as by + symbols. The + symbols show our height grid. Comparing Fig. 2 with Fig. 4 and Fig. 3 with Fig. 5, as well as the different CRD rates in Figs. 4 and 5 clearly shows how a decrease of a brings the CRD emission in successively better agreement with the PRD rates, particularly in the progressively more distant regions behind the shocks. This is due to the validity of the CRD assumption for the Doppler core. The CRD cases with $a = 0$ appear to give rather good approximations to the PRD rates. On the basis of these results we propose the following pseudo-PRD computation procedure for the evaluation of chromospheric line cooling: perform a CRD cooling rate computation with vanishing damping parameter a.

There remain differences between the CRD and PRD rates, particularly in the front shock regions. But it has to be kept in mind that the rates in Figs. 1 to 5 are all plotted on a logarithmic scale. In view of the time-dependent chromospheric energy balance, only the largest cooling rates are important. Our proposed pseudo-PRD method to completely remove the damping wings in a CRD cooling rate calculation thus appears to be a reasonably accurate approximation. Moreover, to compute cooling

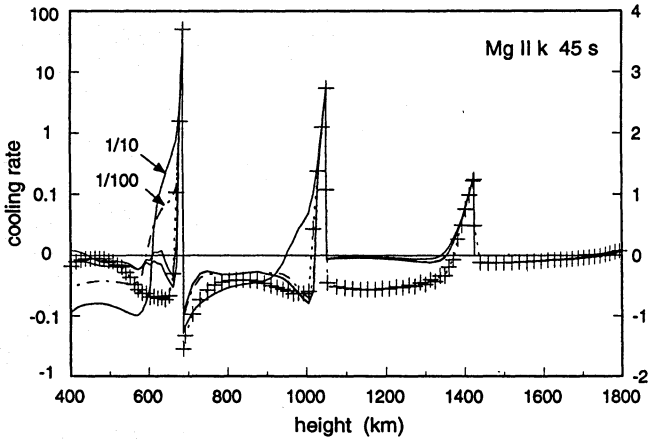

Fig. 5. Same as Fig. 3, however for damping parameters a of Eq. (5) multiplied by factors $1/10, 1/100, 1/1000, 0$. The PRD rates are shown dotted and with + symbols

rates using CRD, represents a saving of computer time by more than an order of magnitude. This computer time, gained by some loss if rigour, is better spent on the computation of additional chromospheric emitters, like e.g. the Lyman α line, because in a time-dependent hydrodynamic calculation not the individual line emission is important, but the total radiation loss from the chromospheric gas elements.

4. Conclusions

From our computations of the Mg II k line cooling rate assuming CRD or PRD both for the Vernazza et al. (1981) solar model C and for solar acoustic wave models we conclude:

1. There are large discrepancies between the CRD and PRD cooling rates. The PRD cooling rates are much smaller than the CRD rates and are much more concentrated in a narrow region behind the shocks.
2. The CRD approximation breaks down progressively, the deeper one penetrates from the surface into the atmosphere.

This is valid both for an external surface like the foot of the transition layer and for internal surfaces such as shocks. Shocks represent internal surfaces because, due to the strong wavelength displacements caused by the velocity jump at the shock discontinuity, they usually have a low opacity region in front, which permits free emission of the hot post shock radiation.

3. Decreasing the damping parameter a of Eq. (5) in a CRD calculation leads to increasingly close agreement with the PRD cooling rates, although small differences remain.

4. We propose a pseudo-PRD method for computing line cooling rates by doing chromospheric line computations in CRD and taking $a = 0$. This method allows to calculate reasonably accurate cooling rates with a much reduced computational effort.

References

Buchholz, B., Hauschildt, P., Rammacher, W., Ulmschneider, P. 1994, Astron. Astrophys. 285, 987

Buchholz, B., Ulmschneider, P. 1995, Astron. Astrophys., in preparation

Caccin, B., Gomez, M.T., Marmolino, C., Severino, G. 1977, Astron. Astrophys. 54, 227

Carlsson, M., Stein, R.F. 1992, Astrophys. J. 397, L59

Cheng, Q.-Q. 1992, Astron. Astrophys. 266, 549

Kalkofen, W., Ulmschneider, P., Schmitz, F. 1984, Astrophys. J. 287, 952

Mihalas, D. 1978, Stellar Atmospheres, 2nd ed., Freeman, San Francisco, USA

Rammacher, W., Ulmschneider, P. 1992, Astron. Astrophys. 253, 586

Ulmschneider, P. 1994, Astron. Astrophys. 288, 1021

Vernazza, J.E., Avrett, E.H., Loeser, R. 1981, Astrophys. J. Suppl. 45, 635